USING CFAR ALGORITHM TO FURTHER IMPROVE A COMBINED THROUGH-WALL IMAGING METHOD

Omar Benahmed daho, Jamal Khamlichi, Olivier Chappe, Bruno Lescalier, Alain Gaugue, Michel Menard

Laboratory of Informatics Image and Interaction (L3i), La Rochelle University, France

ABSTRACT

This paper presents a novel way to increase the detection/localization performance of a through-the-wall radar. In one hand, the false negative detection is reduced by combining the backprojection and the trilateration algorithms. In the other hand, the false positive detection is reduced by using a Constant False Alarm Rate (CFAR) algorithm. Hence, we show that the detection/localization performance of the resulting imaging module is improved. The whole processing pipeline of our ultra wideband (UWB) multistatic pulse radar system is described. We specifically focus on the combination of backprojection and trilateration and the use of CFAR algorithm. Simulations and experiments indicate that our combined method outperforms the other presented method.

Index Terms— ***Through-the-wall imaging pulse radar, UWB, CFAR, backprojection, trilateration.***

1. INTRODUCTION

Through-the-wall (TTW) surveillance has become a strategic research topic because of its outstanding applications in major fields such as antiterrorism and urban security. UWB radar systems are commonly used to detect, locate and track human beings behind dielectric opaque material (concrete, cinderblock, wood…). A system with such abilities is quite useful in hostage-taking situations and antiterrorism operations because, used as a decision aids tool; it assists to establish the best intervention strategies minimizing the human damage and maximizing the effectiveness of the intervention [1]. Over the last years, several products and prototypes have been developed e.g. "Xavers 800" [2] and "RadarVision" [3].

For any TWS system, the used imaging method is the most important component in the processing pipeline. It has to be chosen according to the requirements of the final product. Different approaches dealing with this point are proposed. Backprojection and its different variants [4,5] are widely used because of their simplicity. Moreover, trilateration method [6,7] and Time reversal method (TRM) are also used and even combined with other techniques to outperform their classical versions [8]. Nevertheless, even endowed with an effective imaging method, radar system has to be supplemented by other functionalities. Several post-imaging techniques are investigated in different works such as radar image enhancement, CFAR detection [9, 10] and multiple-target tracking.

The adoption of Constant False Alarm Rate (CFAR) algorithm in short range imaging is judicious. Contrary to the use of one threshold for the whole image, using CFAR can eliminate imaging artefacts due to multi-path effect and validate a distant target with a low intensity signature in order to extract it from the noisy background. This is possible because the data is observed through a window of analysis to determine the local threshold of detection which depends on the positioning with reference to the radar system. In the literature, several well-know versions of CFAR processor exist. The Cell-Averaging CFAR (CA-CFAR) is commonly used. Figure 1 shows the architecture of a CA-CFAR processor for a 1-D signal. Our radar system does not use this processor in this way. The 2D version is used to process the radar images. CA-CFAR models the background as an exponential distribution [11] whose parameters are estimated using the pixels of a reference cell (RC). RC surrounds the cell under test (CUT) *Y*. the guard cell (GC) separates these two cells to avoid that the results being distorted by data from the investigated cell. The values of the pixels in the guard cell are not used in this process. The CUT is considered as target if its power is greater than the average one of the reference cell.

In this paper, we propose a combined backprojection-trilateration imaging method. The combined method has a better localization performance to a detriment of slightly higher false positive detection rate. This latter is reduced using a modified CFAR algorithm.

The remainder of the paper is organized as follow. A succinct description of our radar system prototype and its signal processing is given in Section 2. In Section 3, we propose a novel way to combine backprojection and trilateration algorithms. In Section 4, we present CFAR algorithm. Simulations and experiments results are presented in Section 5. A summary of the results and some extensions are given in Section 6.

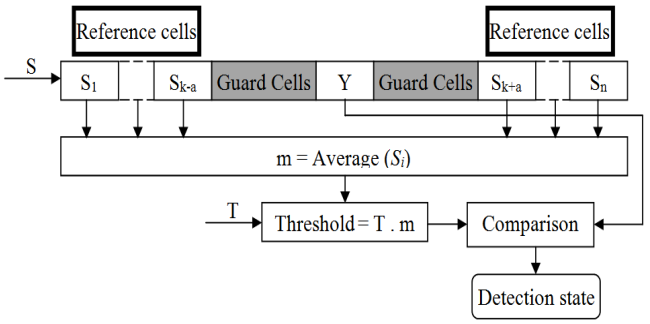

Figure 1. Traditional CA-CFAR processor for 1D signals.

2. THE RADAR SYSTEM DESCRIPTION

A block diagram of the processing steps is shown in figure 2. In our multistatic radar system, an UWB omnidirectional antenna is used as a transmitter. The transmitted signal is an amplified Gaussian pulse, modulating a sinusoidal function. The center frequency is 4.6GHz with a bandwidth of 3.2 GHz. The first version of our prototype employed mechanical sweeping in a bistatic configuration [12]. In the following, we consider three UWB receivers in a multistatic configuration. Their radiation patterns are symmetrical with an opening angle of ±45°.

The acquired signals are preprocessed using usual techniques [13]. Envelope detection with Hilbert transform is used to demodulate received signals. Time zero is determined knowing the positions of the receiving antennas and the time of arrival of the corresponding crosstalk. This latter is eliminated afterwards using a priori crosstalk information. Received signals are denoised to enhance their SNR. Then, the radar imaging algorithm is performed. We use a combined backprojection-trilateration algorithm (cf. Section 3.1-3). A CFAR detection algorithm is used in order to decrease the false positive detection rate (cf. Section 4). TTW Radar image time series are split up to two parts. The first part contains the moving targets whereas the second contains the steady ones. This is done using a moving object segmentation algorithm. This operation helps to apply specific processing on each part. Multiple-target tracking using an extended Kalman filter-based method is applied on the first part (moving targets). Interior walls highlighting using a Radon transform-based method is applied on the second part. At the last, several images showing different kinds of information are displayed notably moving targets, steady targets and the architectural plan of the scene. In the following, we focus on the radar imaging method and how to enhance its detection performance using CFAR detection algorithm.

3. RADAR IMAGING METHOD

Our radar imaging module is mainly based on time-domain backprojection and trilateration algorithms which are well adapted to our pulse radar system.

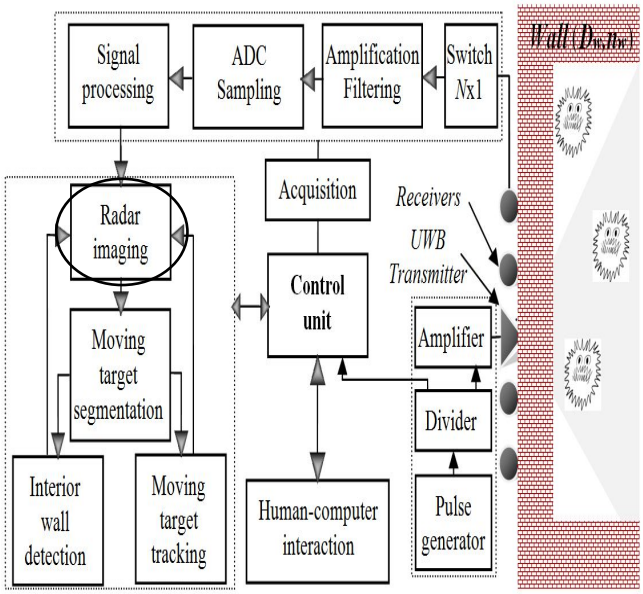

Figure 2. Block diagram of the radar processing pipeline.

The use of only one imaging method is not obligatory. The imaging methods can be combined with each other to outperform their classical versions. Thus, backprojection can be combined with other techniques, e.g. trilateration, in order to get more accurate localization or just to confirm the given information by backprojection. Such a combination can be observed while handling "RadarVision" [3]. In order to combine backprojection and trilateration algorithms, this latter is adapted to multiple-target localization. In the following, the two algorithms are presented separately. We next present how the combination is done.

3.1. Considering the wall effects

The scene under surveillance is represented using a digital image. Hence, times of arrival (*ToA*) for all the image pixels are calculated and stored in the time matrix M_t. The wall effect is taken in consideration during this step. A pixel has as many *ToA* as the number of receivers. Furthermore, M_t is stationary therefore it is calculated only once. However, performing this computation for each pixel is very time-consuming since it involves trigonometric equation resolution. A simpler propagation model should be used. If we consider Snell's pattern of refraction, then we can make the assumption that the traveled path by the wave in the wall is roughly equal to the wall thickness (D_w). Consequently, time delay caused by TTW round-trip propagation is given by Eq. 1. It can be seen that through Eq.1 that t_{delay} does not depend on the position of the pixel. This approximation gives close results to the more accurate methods.

$$t_{delay} = 2D_w\,(n_w - 1)/c \qquad (1)$$

where, c is the speed of light in the air and n_w is the refractive index of the wall. For non-magnetic material-made walls (e.g. Plasterboard, brick and concrete), n_w is calculated using only its permittivity.
In order to compensate the delay caused by the presence of the wall, t_{delay} should be added to all the values of the time matrix using Eq.2. Otherwise, a shift of t_{delay} can be directly performed on the received signals if the original M_t is used.

$$ToA_{ij} = M_t(i,j) + t_{delay} \quad (2)$$

Eliminating the time delay compensates partially the wall effects. If we deal with this issue in frequency domain, the compensation will be almost accurate. The attenuation and the phase angle difference of the received signals depend on frequency. Consequently, the frequency components are not delayed in the same way. However, time-domain processing gives a fast and reasonably good approximation of the real time-delay.

3.2. Backprojection

This algorithm [4] generates an image which represents the scene under surveillance. Each pixel of this image corresponds to a given dimension (e.g. *5cm*). The intensity η of the pixel (i,j) is obtained by using equation (3). For each pixel, with a time of flight TOA_{ij}, and for each received signal (from antenna n) s_n, a correlation coefficient (ρ_n) is computed along the effective width of the impulse (p_w) by using equation (4). s_{refi}, i=1,2 are the signals issued from two auxiliary referential receivers. The final pixel intensity is the mean of all intensities.

$$\eta(i,j) = \frac{1}{N}\sum_{n=1}^{N} \rho_n(i,j) \quad (3)$$

$$\rho_n(i,j) = \frac{1}{p_w}\sum_{p_w} s_n(t_{ij}) * s_{ref1}(t_{ij}) * s_{ref2}(t_{ij}) \quad (4)$$

where, N is the number of receiving antennas, p_w is the pulse width and t_{ij} is the duration of the round-trip from the transmitter to the pixel *(i,j)* and back to the receiver n.

3.3. Multiple-target trilateration

The multiple-target localization problem of trilateration is dressed using minimization of target position root mean square (RMS). After detecting the echo of the targets in the signals, all possible target positions are obtained using the traditional trilateration algorithm [7]. Among these positions, the false ones are eliminated according to the value of the corresponding RMS (Eq. 5) compared to a threshold value. RMS measures the similarity between the temporal information and the spatial information of the detected targets. Choosing a suitable threshold leads to a good localization performance.

$$RMS = \sqrt{\frac{1}{N}\sum_{n=1}^{N}(c.ToA_n - (TTd + TRd_n))^2} \quad (5)$$

where, *ToA* is the Time of Arrival of the pixel *(x,y)*, *TTd* is the transmitter-pixel distance, *TRd* is the pixel-receiver distance and *c* is the speed of light in the air.

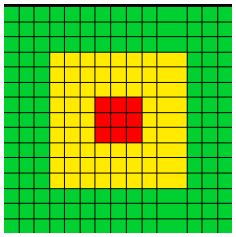

Figure 3. Traditional 2D CFAR window.
CUT; GC; RC

3.4. The combined Imaging method

If we try to simply add the results of backprojection and trilateration, then the detection performance would not be good. Consequently, the combination is done by first matching the localization results of backprojection with those of trilateration. Thereafter, isolated targets detected by backprojection are deleted depending on their clutter strength. Whereas, the ones detected by trilateration are deleted depending on the value of RMS. This method outperforms the traditional ones in regards of the false negative detection rate at a cost of an increased false positive detection rate.

4. INCORPORATING CFAR ALGORITHM

Although the combined imaging method has a greater detection rate than the traditional methods, its false positive detection rate is slightly higher. In order to decrease it, a modified CFAR detection algorithm is performed on TTW radar image time series.
Traditionally, we scan the images with a sliding 2D CFAR window. The scan is done pixel by pixel throughout the entire image. The edges have a special processing. In Figure 3, we show the three different cells as presented in section I. The CUT is the inner (red) part. It should cover the target signature. The RC is the outer (green) part. It should contain pixels from the background. GC is the third (yellow) part. It separates the two first parts and prevents from using pixels with high intensity belonging to the target's side-lobes [14]. The sizes of these cells strongly depend on the radar system features such as bandwidth, angular resolution and the performed signal processing.
The energy of the CUT ($Y_E = \sum_{(i,j)\in CUT} CUT^2(i,j)$) and the RC ($X_E = \sum_{(i,j)\in RC} RC^2(i,j)$) are computed. These two energies are compared. According to the value of the CUT energy to the RC energy ratio, the CUT will be or not considered as target. Therefore, the RC energy should not be close to zero in order not to get too much false positive detection and to prevent division by zero problems. Equation 6 defines the CFAR test. T is a suitable threshold which can be chosen according to the images characteristics. $\varphi(i,j)$ is the corresponding pixel to the center of the CUT in the detection image.

$$\varphi(i,j) = \begin{cases} 1 & Y_E/X_E \geq T \\ 0 & otherwise \end{cases} \quad (6)$$

The traditional CFAR detection was implemented. However, for real-time and detection performance considerations, several modifications were made. The used CFAR window as well as the CFAR test has undergone significant changes. The proposed CFAR algorithm outperforms the traditional one.

5. EXPERIMENTS AND RESULTS

In this section, obtained simulation and experiment results is shown, compared and discussed. We have developed a 3.2GHz multistatic pulse radar system. The prototype employs a computer on which the entire processing pipeline is implemented. In the following, we present obtained results on simulated data and real data. Both sets were processed with the presented algorithms. In the following, the unit of the coordinates is always meter. The used scenario for evaluating the combined imaging method is as follows: one target is going from point *(-2,0.5)* to point *(2,1.5)* and another target is going from point *(2,0.5)* to point *(-2,1.5)*. The two targets have the same pace and reflectivity coefficient. Another target stays all the time long at *(0, 3.5)*. On the frame shown at figures 4, 5 and 6 (left), the three targets were expected to be at *(1.8, 1.45)*, *(-1.8, 1.45)* and *(0, 3.5)* respectively.

For real experiments, the scene under surveillance is a *(4, 3.5)* rectangular room where a metallic target was moved in a zigzag. On the frame shown at figures 4, 5 and 6 (right), the target was expected to be at *(-0.2, 1.6)* and the interior wall is at *3.5*.

The Cartesian coordinates are shown on the figures. We consider the transmitter as the origin of coordinates. The right side has positive abscissas whereas the left side has negative abscissas. For both cases, targets were sensed within 101 frames through a 13cm plasterboard wall. The complex dielectric constant of the wall is $\varepsilon = 6 - i.0.6$ [15]. It is considered invariant throughout the operating bandwidth.

5.1. Combined imaging method without CFAR

Backprojection and trilateration algorithms were combined in an attempt to increase the detection performance. For both individual methods, detection rates undergo significant variation within the SNR scope. Combining the two algorithms decreases considerably the false negative detection rate whereas the false positive detection rate is slightly higher than the one obtained using only the backprojection algorithms. Moreover, detection rates are relatively constant throughout the large SNR scope.

Figure 4 shows the radar images obtained by simulation and with real experiments. False positive detected targets can be seen especially at the back of the room where the SNR of the received signals is the lowest.

	SNR (dB)	0	3	10	15
Backprojection	PD (%)	79.54	83.17	84.48	87.13
	ANFA	1.45	0.81	0.72	0.62
Multiple-target Trilateration	PD (%)	47.85	57.09	73.27	76.24
	ANFA	0.63	0.26	0.32	0.25
BP+MTTL	PD (%)	85.15	88.45	93.73	95.38
	ANFA	2.09	1.07	1.04	0.87
Combination without CFAR	PD (%)	71.95	81.52	90.76	94.72
	ANFA	1.15	0.71	0.94	0.79
Combination using CFAR	PD (%)	**71.95**	**81.52**	**90.76**	**94.72**
	ANFA	**0.67**	**0.46**	**0.34**	**0.37**

Table 1. Detection performance of the presented imaging methods (3 targets, 101 frames).
PD: Probability of detection; BP: Backprojection;
ANFA: Average number of false alarm;
MTTL: Multiple-target Trilateration.

Table 1 shows the detection rates of the presented methods at different noise levels. The ANFA is the Average number of false positive detected target. The results depend strongly on the number of the targets and how they move in the scene under surveillance. Simply adding (BP+TL) the results of the two methods does not give good results in terms of false detection rate, especially at low SNR values. That shows the advantage of our combination.

5.2. Using CFAR algorithm

CFAR detection algorithm is incorporated in the combined imaging method. It helps to further enhance the detection performance by reducing the false positive detection rate. Figure 5 shows the detected target using our CFAR detection algorithm. The false alarms are then suppressed using image processing based on the fast hybrid grayscale geodesic reconstruction algorithm described in [16].

Figure 6 shows the radar image with only the detected target after suppression of the false alarms.

Moreover, through table 1, it can be seen that using CFAR algorithm decreases effectively the false positive detection rate. For low values SNR, the performance of this method is equivalent to the one of backprojection. Therefore, efficient signal processing has to be performed in order to fully take advantage of this combination.

6. CONCLUSION

After dealing with the trilateration multiple-target problem, a combined backprojection-trilateration imaging method has been presented. The results show that the combination of these two methods eliminates their limitations and yields an accurate imaging method in regards of the false negative detection rate. However, the obtained false detection rate values of this method do not fit with our aim of detection effectiveness. Therefore, CFAR detection algorithm was incorporated into the imaging block, in an attempt to decrease the false alarms.

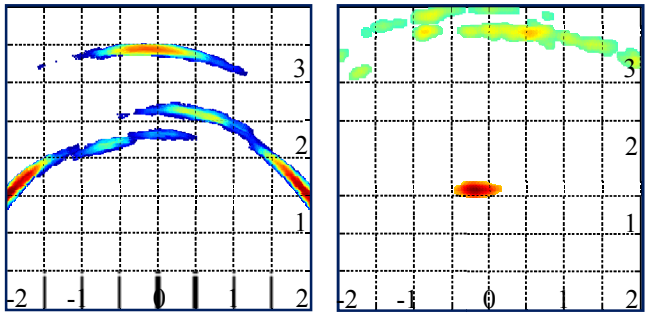

Figure 4. Detected targets using the combined method without CFAR.
left: simulation; right: real data

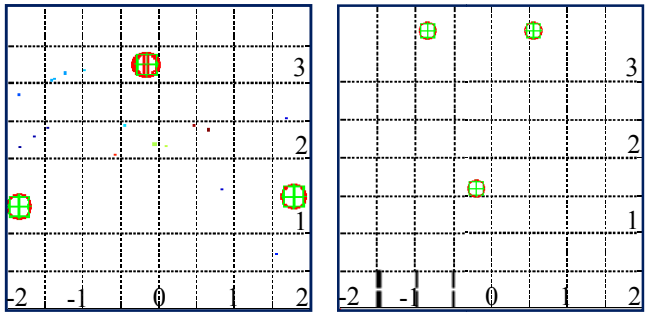

Figure 5. Detected targets using CFAR on the images in figure 4.
left: simulation; right: real data

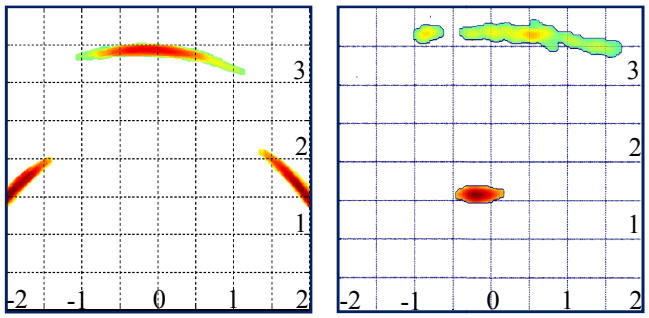

Figure 6. The resulting images after incorporating CFAR.
left: simulation; right: real data

The global imaging method outperforms both backprojection and trilateration with regards to false positive and false negative detection. This should increase the effectiveness of the subsequent processing steps.
In the future works, different kind of walls will be considered. Also, information obtained from the subsequent processing steps e.g. moving targets segmentation and multiple-target tracking will be used to further improve the presented imaging method.

7. ACKNOWLEDGE

This work was undertaken with help of a specific funding program FEDER n° 31260 – European Regional Development Fund – from the European Union.

8. REFERENCES

[1] E. J. Baranoski, "Through-wall imaging: Historical perspective and future directions", J. Franklin Inst., Vol. 345, pp. 556-569, 2008.

[2] A. Beeri, D. Gazelle and M. Divald, "Through Wall Imaging device", World Patent WO 2007/029226 A2 March, 15 2007.

[3] Radar Vision, Time Domain Corporation [online], www.timedomain.com.

[4] Lane, R.O. & Hayward, S.D. 2007. Detecting personnel in wooded areas using MIMO radar, IET International Conference on Radar Systems, Edinburgh, UK, 15-18 October 2007.

[5] M. Soumekh, "Synthetic Aperture Radar Signal Processing with MATLAB Algorithms", New York, John Wiley and Sons, Inc. 1999.

[6] F. Ahmad and M. G. Amin, "A noncoherent approach to radar localization through unknown walls", Proc. IEEE Conf. Radar, pp. 583-589 , 2006.

[7] X. W. Zhao, A. Gaugue, C. Lièbe, J. Khamlichi, and M. Ménard, "Through-the-wall detection and localization of a moving target with a bistatic UWB radar system", EURAD, Paris, pp. 204-207, Oct 2010.

[8] W. Zheng, Z. Zhao, and Z. Nie, "Application of TRM in the UWB through wall radar", Progress In Electromagnetics Research, 87, pp. 279-296, 2008.

[9] Chul H. Jung, Woo Y. Song, Soo H. Rho, Jung Kim, Jung T. Park and Young K. Kwag, "Double-Step Fast CFAR Scheme for Multiple-target Detection in High Resolution SAR Images", in Radar Conference , pp. 1172-1175, IEEE, 2010.

[10] Gun Rongbing and Wang Jianguo, "Distribution-based CFAR detectors in SAR images ", Journal of Systems Engineering and Electronics, pp. 717-721, Dec 2006.

[11] N. N. Liu and J. W. Li. " A New Detection Algorithm Based On Cfar For Radar Image With Homogeneous Back-Ground ", Progress In Electromagnetics Research C, Vol. 15, pp. 13-22, 2010.

[12] C. Liebe, A. Gaugue, X. Zhao, J. Khamlichi, M. Ménard, "A through wall UWB RADAR with mechanical sweeping system", Microwave Conference, 2009. EuMC 2009. European, pp. 1634-1637, Italie, 2009.

[13] C. Liebe, A. Gaugue, J. Khamlichi, M. Ménard, J-M. Ogier, "UWB Radar: Mechanical Scanning and Signal Processing for Through-the-Wall Imaging", Ultra-Wideband, Short Pulse 9, pp. 385-393, 2010.

[14] A. Martone, K. Ranney and R. Innocenti, "Automatic through the wall detection of moving targets using low-frequency ultra-wideband radar", In Proc. IEEE Inter. Radar Conf., pp. 39-43, May 2010.

[15] E. Damosso, "Digital Mobile Radio towards Future Generation Systems", Final Report, EUR 18957, ed. COST 231, 1999.

[16] L. Vincent., "Morphological Grayscale Reconstruction in Image Analysis: Applications and Efficient Algorithms," IEEE Transactions on Image Processing, Vol. 2, No. 2, pp. 176-201, April, 1993.